



Contents lists available at ScienceDirect

## Metabolism Clinical and Experimental

journal homepage: [www.metabolismjournal.com](http://www.metabolismjournal.com)

## Absence of AGPAT2 impairs brown adipogenesis, increases IFN stimulated gene expression and alters mitochondrial morphology

Pablo J. Tapia<sup>a,1</sup>, Ana-María Figueroa<sup>a,1</sup>, Verónica Eisner<sup>b</sup>, Lila González-Hódar<sup>a</sup>, Fermín Robledo<sup>a</sup>, Anil K. Agarwal<sup>c</sup>, Abhimanyu Garg<sup>c</sup>, Víctor Cortés<sup>a,\*</sup><sup>a</sup> Department of Nutrition, Diabetes and Metabolism, School of Medicine, Pontificia Universidad Católica de Chile, Santiago 8330024, Chile<sup>b</sup> Department of Cellular and Molecular Biology, School of Biological Sciences, Pontificia Universidad Católica de Chile, Santiago 8331150, Chile<sup>c</sup> Division of Nutrition and Metabolic Diseases, Department of Internal Medicine, University of Texas Southwestern Medical Center, Dallas, TX 75390, United States of America

## ARTICLE INFO

## Article history:

Received 6 May 2020

Accepted 10 August 2020

## Keywords:

AGPAT2

Brown adipose tissue

Adipogenesis

Type I interferon

Mitochondria

## ABSTRACT

**Background:** Biallelic loss of function variants in *AGPAT2*, encoding 1-acylglycerol-3-phosphate O-acyltransferase 2, cause congenital generalized lipodystrophy type 1, a disease characterized by near total loss of white adipose tissue and metabolic complications. *Agpat2* deficient (*Agpat2*<sup>-/-</sup>) mice completely lacks both white and interscapular brown adipose tissue (iBAT). The objective of the present study was to characterize the effects of AGPAT2 deficiency in brown adipocyte differentiation.

**Methods:** Preadipocytes obtained from newborn (P0.5) *Agpat2*<sup>-/-</sup> and wild type mice iBAT were differentiated into brown adipocytes, compared by RNA microarray, RT-qPCR, High-Content Screening (HCS), western blotting and electron microscopy.

**Results:** 1) Differentiated *Agpat2*<sup>-/-</sup> brown adipocytes have fewer lipid-laden cells and lower abundance of *Pparγ*, *Pparα*, *C/ebpα* and *Pgc1α*, both at the mRNA and protein levels, compared those to wild type cells. *Prmd16* levels were equivalent in both, *Agpat2*<sup>-/-</sup> and wild type, while *Ucp1* was only induced in wild type cells, 2) These differences were not due to lower abundance of preadipocytes, 3) Differentiated *Agpat2*<sup>-/-</sup> brown adipocytes are enriched in the mRNA abundance of genes participating in interferon (IFN) type I response, whereas genes involved in mitochondrial homeostasis were decreased, 4) Mitochondria in differentiated *Agpat2*<sup>-/-</sup> brown adipocytes had altered morphology and lower mass and contacting sites with lipid droplets concomitant with lower levels of Mitofusin 2 and Perlipin 5.

**Conclusion:** AGPAT2 is necessary for normal brown adipose differentiation. Its absence results in a lower proportion of lipid-laden cells, increased expression of interferon-stimulated genes (ISGs) and alterations in mitochondrial morphology, mass and fewer mitochondria to lipid droplets contacting sites in differentiated brown adipocytes.

© 2020 Elsevier Inc. All rights reserved.

**Abbreviations:** ACAA2, acetyl-Coenzyme A acyltransferase 2; ADIPOQ, adiponectin; AGPAT2, 1-acylglycerol-3-phosphate O-acyltransferase-2; C/EBPα, CCAAT/enhancer-binding protein alpha; C/EBPβ, CCAAT/enhancer-binding protein beta; CIDEA, cell death-inducing DNA fragmentation factor alpha-like effector A; CGL, congenital generalized lipodystrophy; COX7A1, cytochrome c oxidase subunit 7A1; COX8B, cytochrome c oxidase subunit 8B; CtBP, C-terminal-binding protein-1; DDX58, DEAD (Asp-Glu-Ala-Asp) box polypeptide 58; DHX58, DEXH (Asp-Glu-X-His) box polypeptide 58; EBF2, early B cell factor 2; EFGP, enhanced green fluorescent protein; FABP4, fatty acid binding protein 4; GFP, green fluorescent protein; GO, gene ontology; HSP70, Heat shock 70 kDa protein; iBAT, Interscapular brown adipose tissue; IBMX, 3-isobutyl-1-methylxanthine; IFI204, Interferon-activable protein 204; IFI44, Interferon-induced protein 44; IFIH1, interferon induced with helicase C domain 1; IFIT1, interferon-induced protein with tetratricopeptide repeats 1; IFN, interferon; IRF, interferon regulatory factor; ISGs, interferon-stimulated genes; iWAT, inguinal white adipose tissue; MFN2, mitofusin 2; mtDNA, mitochondrial DNA; nDNA, nuclear DNA; OAS1G, 2'-5' oligoadenylate synthetase 1G; *Nd4*, Mitochondrially encoded NADH:Ubiquinone Oxidoreductase Core Subunit 4; OASL2, 2'-5'-oligoadenylate synthase-like protein 2; PA, phosphatidic acid; PGC1α, proliferator-activated receptor gamma coactivator 1-alpha; PLIN1, perilipin 1; PLIN5, perilipin 5; PPARα, peroxisome proliferator-activated receptor Alpha; PPARγ, peroxisome proliferator-activated receptor gamma; PRDM16, PRD1-BF1-RIZ1 homologous domain containing 16; PREF1, preadipocyte factor 1; RLRs, retinoic acid-inducible gene-1-like receptors; SCAD, short-chain acyl-CoA dehydrogenase; SSMD, strictly standardized mean difference; STAT, signal transducer and activator of transcription; SVF, stromal vascular fraction; TOM20, Translocase of outer membrane 20 kDa subunit; T3, triiodothyronine; UCP1, uncoupling protein 1; USP18, Ubl carboxyl-terminal hydrolase 18; VLCAD, very long-chain acyl-CoA dehydrogenase; ZFP423, zinc finger protein 423.

\* Corresponding author at: Department of Nutrition, Diabetes and Metabolism, School of Medicine, Pontificia Universidad Católica de Chile, Av. Libertador Bernardo O'Higgins 340, Santiago 8331150, Chile.

E-mail addresses: [pijtapia@uc.cl](mailto:pijtapia@uc.cl) (P.J. Tapia), [aifigueroa@uc.cl](mailto:aifigueroa@uc.cl) (A.-M. Figueroa), [veisner@bio.puc.cl](mailto:veisner@bio.puc.cl) (V. Eisner), [ldgonzal@uc.cl](mailto:ldgonzal@uc.cl) (L. González-Hódar), [farobled@uc.cl](mailto:farobled@uc.cl) (F. Robledo), [anil.agarwal@utsouthwestern.edu](mailto:anil.agarwal@utsouthwestern.edu) (A.K. Agarwal), [abhimanyu.garg@utsouthwestern.edu](mailto:abhimanyu.garg@utsouthwestern.edu) (A. Garg), [vcortesm@uc.cl](mailto:vcortesm@uc.cl) (V. Cortés).

<sup>1</sup>These authors contributed equally and must be both considered as first authors.

## 1. Introduction

Congenital generalized lipodystrophy (CGL) is a rare autosomal recessive disease characterized by severe lipodystrophy since birth, insulin resistance, early onset diabetes and hepatic steatosis [1–3]. Type 1 CGL due to biallelic loss of function variants in *AGPAT2*, is the commonest subtype, followed by type 2, type 4 and type 3 CGL, due to *BSCL2*, *CAVIN1* and *CAV1* variants, respectively [4]. *AGPAT2* encodes 1-acylglycerol-3-phosphate O-acyltransferase-2, that converts lysophosphatidic acid (LPA) into phosphatidic acid (PA) in the *de novo* glycerophospholipid synthesis pathway [5–7]. Mice lacking *Agpat2* (*Agpat2*<sup>-/-</sup>) recapitulate nearly all clinical features of CGL [2,8], however, they are born with both white and interscapular brown adipose tissue detectable by morphological and molecular methods [9]. In these animals, adipose tissue completely degenerates during the first 6 days after birth, as a result of selective adipocyte death and inflammatory infiltration [9]. The mechanisms of adipose tissue destruction in *Agpat2*<sup>-/-</sup> mice remain unknown.

In our previous work, we found that the lack of *Agpat2* results in failed adipogenesis in mouse embryonic fibroblasts [9] and preadipocytes differentiated into white adipocytes [10]. The consequences of *Agpat2* deficiency in brown adipocyte differentiation have not been described.

Adipogenesis is regulated by multiple transcriptional regulators [11–13], that ultimately promotes expression of genes involved in cell differentiation, lipid accretion [14,15], lipid droplet (LD) formation and function and secretion of protein hormones known as adipokines [16], whereas simultaneously prevent the expression of genes implicated in the maintenance of stemness or the commitment into non-adipocyte phenotypes [11]. Additionally, brown adipogenesis involves repression of genes implicated in skeletal muscle differentiation and activation of genes implicated in mitochondrial biogenesis and thermogenesis [13]. Brown adipocytes have abundant expression of uncoupling protein 1 (*Ucp1*) [17–20], which is considered a *bona fide* marker for brown adipocyte phenotype [13,21].

In this study we aimed to characterize the cellular and molecular impact of *AGPAT2* deficiency in brown adipocyte differentiation. For this, we used a model of *in vitro* brown adipogenesis with preadipocytes harvested from the stromal vascular fraction of the interscapular brown adipose tissue (iBAT) of *Agpat2*<sup>-/-</sup> mice.

## 2. Materials and methods

### 2.1. Maintenance and generation of mice

*Agpat2*<sup>-/-</sup> mice were generated and genotyped as previously described [8]. The *Agpat2*<sup>+/+</sup> (wild type) and *Agpat2*<sup>-/-</sup> mice were generated by mating of *Agpat2*<sup>+/-</sup> progenitors. The mouse strain *Agpat2*<sup>+/-</sup>/*Zfp423*<sup>GFP</sup> was generated by crossing *Agpat2*<sup>+/-</sup> and *Zfp423*<sup>GFP</sup> (B6; FVB-Tg (*Zfp423*-EGFP)7Brsp/J, 19381, Jackson Laboratory). The *Agpat2*<sup>+/-</sup>/*Zfp423*<sup>GFP</sup> mice was then used for the generation of *Agpat2*<sup>+/+</sup>/*Zfp423*<sup>GFP</sup> and *Agpat2*<sup>-/-</sup>/*Zfp423*<sup>GFP</sup> mice. Mice were maintained with 12 h light and dark cycles. All animal experiments were performed as approved by Pontificia Universidad Católica de Chile committee for animal safety and bioethics and performed following the principles of Helsinki Declaration.

### 2.2. iBAT preadipocytes and brown adipogenic differentiation

Newborn pups (P0.5) from *Agpat2*<sup>+/+</sup> and *Agpat2*<sup>-/-</sup> were euthanized by decapitation and iBAT was retrieved by surgical resection. Tissues from individual mice were processed, cultured, genotyped and studied by separate. Only microarray analysis was based on pooled RNA from animals of the same age and genotype. For generating stromal vascular fraction (SVF), iBAT was washed in ice-cold phosphate-buffered saline (PBS), minced with surgical scissors and digested with

0.2% type II collagenase (17101015, Gibco) prepared in 25 mM KHCO<sub>3</sub>, 12 mM KH<sub>2</sub>PO<sub>4</sub>, 1.2 mM MgSO<sub>4</sub>, 4.8 mM KCl, 120 mM NaCl, 1.2 mM CaCl<sub>2</sub>, 5 mM glucose, 2.5% BSA and 1% penicillin/streptomycin, at pH 7.4 for 45 min at 37 °C. The digest was passed through a 100 µm mesh and 400 µL ammonium-chloride-potassium lysis buffer (A1049201, Gibco) was added for 4 min. The resulting cell suspension was mixed with 1 mL of culture medium (DMEM-F12 (12400024, Gibco), 10% FBS (16000044, Gibco), 1% antibiotic/antimycotic solution (15240062, Gibco), pH 7.2), and centrifuged at 300 ×g for 5 min. The resulting pellet was resuspended in 1 mL of culture medium, filtered in a 40 µm mesh, washed as in the previous step and seeded in plastic dishes (11.4 cm<sup>2</sup>). After reaching confluence, the cells were trypsinized and seeded (1:6 diluted) in plastic dishes. An aliquot of cells was used for genotyping using a previously published protocol [8]. This latter cell culture expansion was repeated once and after reaching confluence brown adipogenesis was induced with a cocktail containing 500 nM dexamethasone (D4902, Sigma-Aldrich), 125 nM indomethacin (17378, Sigma-Aldrich), 0.5 mM IBMX (15879, Sigma-Aldrich), 5 µM rosiglitazone (R2408, Sigma-Aldrich), 1 nM T3 (T6397, Sigma-Aldrich) and 20 nM insulin (I3536, Sigma-Aldrich). After 72 h of induction, cells were maintained in regular medium supplemented with 20 nM insulin, 5 µM rosiglitazone and 1 nM T3.

### 2.3. Immunofluorescence analysis

*Agpat2*<sup>-/-</sup> and wild type mice iBAT preadipocytes were seeded and differentiated in optical bottom 96-well plastic plates. After differentiation, the cells were fixed with 4% paraformaldehyde (158127, Sigma-Aldrich) for 20 min and washed 3 times with ice-cold PBS, permeabilized with 0.1% Triton X-100 (T8787, Sigma-Aldrich) for 15 min and blocked with 3% fish gelatin (G7765, Sigma-Aldrich) by 1 h at room temperature. The cells were washed 3 times with PBS and incubated with primary antibodies anti-PPAR $\gamma$  1:200 (2443, Cell Signaling), Perilipin-1 1:200 (9349, Cell Signaling), (1% BSA/PBS) overnight at 4 °C in a humid chamber. After washing 3 times with PBS, cells were incubated with a secondary goat anti-rabbit IgG (H + L) highly cross-adsorbed secondary antibody labeled with Alexa Fluor 647 (A-21245, Thermo Fisher) (1:1000, 1% BSA/PBS) for 1 h at room temperature. Cellular nuclei were stained with Hoechst 33342 (H21492, Thermo Fisher, 1 µg/mL) and lipid droplets were labeled with BODIPY (D3922, Thermo Fisher, 1 µg/mL) for 30 min at room temperature.

### 2.4. Quantitative fluorescence microscopy and automated imaging analysis

*Agpat2*<sup>-/-</sup> and wild type mice iBAT preadipocytes were seeded in optical-bottom 96-well plastic plates and differentiated and processed as indicated for confocal immunofluorescence microscopy. Microscopy images were acquired with Cytation 5 Cell Imaging Multi-Mode Reader system and analyzed with Gen 5 Image Prime software (BioTek Instruments, Inc., Winooski, VT, USA). 16 images (20× magnification) were acquired per well using blue (Ex 377, Em 447), green (Ex 469, Em 525) and far red (Ex 628, Em 685) color channels. First, cells were segmented by the cell nucleus (primary mask, blue color). Next, a secondary mask was generated with a radial distance of 5 µm from the nucleus. The intensity of green fluorescence in the secondary mask was measured to identify the cells with lipid droplets. Finally, red fluorescence intensity in the primary mask was measured for nuclear markers, and fluorescence intensity in the secondary mask was measured to quantify cytoplasmic markers. Cells were considered as positive or negative for markers by Strictly Standardized Mean Difference (SSMD) [22] (Supplementary Fig. S1).

### 2.5. Western blotting

Differentiated brown adipocytes or iBAT were lysed in RIPA buffer (89901, Thermo Scientific) supplemented with protease (87786,

Thermo Scientific) and phosphatase (78420, Thermo Scientific) inhibitors. Lysates were sonicated on ice and centrifuged at 14,000 ×g for 15 min at 4 °C. 20–25 µg of proteins in the supernatants were mixed with Lane Marker Reducing Sample Buffer (39000, Thermo Scientific) and resolved in 10–12% SDS-polyacrylamide gel electrophoresis. Subsequently, they were electrotransferred onto PVDF membranes (1620177, BioRad). Membranes were blocked with 3% BSA/0.1% Tween 20 (1706531, BioRad) in Tris phosphate buffer/0.1% Tween 20 (TBS-T) for 1 h and incubated with primary anti-Tubulin 1:5000 (ab6046, Abcam), anti-Actin 1:5000 (A2066, Sigma-Aldrich), anti-Vinculin 1:1000 (sc-25336, Santa Cruz), anti-HSP70 1:1000 (sc-32239, Santa Cruz), anti-PPAR $\gamma$  1:1000 (2443, Cell Signaling), anti-PRDM16 1:400 (ab106410, Abcam), anti-C/EBP $\beta$  1:1000 (3087, Cell Signaling), anti-UCP1 1:400 (ab10983, Abcam), anti-PREF1 (2069, Cell Signaling), anti-GFP (2956, Cell Signaling) or anti-PGC1 $\alpha$  1:50 (sc-13067, Santa Cruz), anti-TOM20 1:1000 (42406, Cell Signaling), anti-SCAD 1:1000 (sc-365953, Santa Cruz), anti-VLCAD 1:1000 (sc-376239, Santa Cruz), anti-ACAA2 1:1000 (sc-100847, Santa Cruz) and anti-MFN2 1:1000 (100560, Santa Cruz) primary antibodies (diluted in 1% BSA or 5% milk) overnight at 4 °C. Membranes were washed with TBS-T and incubated with a secondary antibody conjugated with horseradish peroxidase (HRP) for 2 h at room temperature. The membranes were visualized by chemiluminescence using C-DiGit Blot Scanner (Licor) or G:Box (Syngene). Values were normalized to actin, tubulin, vinculin or HSP70 levels.

## 2.6. RT-qPCR and RNA microarray

The total RNA was extracted from differentiated brown adipocytes with Trizol (15596018, Invitrogen) according to manufacturer's instructions. RNA integrity, concentration and purity were determined by gel electrophoresis and spectrophotometry analysis by (ND-1000 Spectrophotometer, NanoDrop, Wilmington, USA), respectively. 2 µg of RNA were treated with TURBO DNA-free™ Kit (AM1907, Invitrogen) for elimination of contaminating DNA. Subsequently, cDNA was generated with High-Capacity cDNA Reverse Transcription Kit (4368814, Applied Biosystems). Relative expression levels of individual mRNAs were determined with  $\Delta\Delta$ Ct method using *36b4* as reference gene [23]. Primers sets are shown in Supplemental Table A3.

For microarray analysis, total RNA concentration, purity and integrity were evaluated with spectrophotometry (NanoDrop, Wilmington, USA) and Agilent 2100 Bioanalyzer (Agilent Technologies, Palo Alto, USA), respectively. cDNA was synthesized using the GeneChip WT (Whole Transcript) Amplification kit as described by the manufacturer. Sense cDNA was fragmented and biotin-labeled with TdT (terminal deoxynucleotidyl transferase) using the GeneChip WT Terminal labeling kit. Approximately 5.5 µg of labeled DNA target were hybridized to Affymetrix® GeneChip™ at 45 °C for 16 h. Hybridized arrays were washed and stained on a GeneChip Fluidics Station 450 and scanned on a GCS3000 Scanner (Affymetrix). Signal values were computed using the Affymetrix® GeneChip™ Command Console software. All Statistical test and visualization of differentially expressed genes was conducted using R statistical language v. 3.1.2 (<http://www.r-project.org>). Gene Ontology (GO) analysis was performed using Gene Ontology resource (<http://geneontology.org/>) [24,25].

## 2.7. Electron microscopy

Differentiated brown adipocyte were grown and differentiated in Thermanox plastic coverslip (174950, Thermo Scientific). Next, the cells were fixed with 2% glutaraldehyde for 2 h, immersed in 1% OsO<sub>4</sub>, dehydrated with ethanol and infiltrated in Epon. Ultra-fine sections were obtained by ultramicrotome (80 nm). Grids were visualized in Phillips Tecnai 12 electron microscope at Advanced Microscopy Facility UMA-UC, at Pontificia Universidad Católica de Chile.

## 2.8. Mitochondrial DNA quantification

Total DNA from differentiated brown adipocytes was isolated with Wizard® Genomic DNA Purification kit (A1120, Promega). Quantitative real-time PCR was performed in triplicate in 96-well plates in StepOnePlus™ thermocycler (Applied Biosystems) using Fast SYBR™ Green Master Mix (4385612, Applied Biosystems) and 10 ng of total DNA. The relative abundance of the mitochondrial DNA encoded gene *Nd4* relative to the nuclear DNA encoded gene *Gapdh* was determined according to the 2- $\Delta\Delta$ Ct method. Primers sets are shown in Supplemental Table A3.

## 2.9. Statistics

Two-way ANOVA followed by Sidak's multiple comparisons test was performed using GraphPad Prism version 6.01 for Windows (GraphPad Software, La Jolla California, USA). Data were expressed as mean  $\pm$  SD. \* $p < 0.05$  denote statistically significant difference between *Agpat2*<sup>-/-</sup> and wild type cells at the same day of differentiation, and # $p < 0.05$  denotes statistically significant difference between times of differentiation within each genotype.

## 3. Results

### 3.1. Differentiated *Agpat2*<sup>-/-</sup> brown adipocytes have a lower proportion of lipid laden cells and fail to express *Ucp1*

*Agpat2*<sup>-/-</sup> mice are born with white and brown adipocytes but whole-body adipose tissue completely degenerates as soon as the sixth day of postnatal life, leading to total lipodystrophy [9]. We previously showed that AGPAT2 is required for normal adipogenic differentiation of white adipocytes [9]. To determine the importance of AGPAT2 in brown preadipocytes adipogenesis, we differentiated SVF from the iBAT of *Agpat2*<sup>-/-</sup> mice and determined the abundance of cells accumulating neutral lipids with an automatized imaging system at different days after adipogenic induction. As shown in Fig. 1A and B, whereas ~80% of differentiated wild type SVF cells had lipid droplets (LDs) at the 5th day after adipogenic induction, the proportion of *Agpat2*<sup>-/-</sup> cells laden with LDs was ~50% lower.

At the molecular level, the mRNA abundance of Perilipin1 (*Plin1*), Adiponectin (*Adipoq*) and Cidea was lower in differentiated *Agpat2*<sup>-/-</sup> compared to wild type brown adipocytes (day 5 of differentiation), likely as a consequence of a lower abundance of lipid droplets in these cells and suggesting impaired adipogenic (Fig. 1C-E). AGPAT2 mRNA levels were progressively increased during brown adipogenesis in wild type cells, being ~250–300-fold higher at days 5 and 7 of differentiation in comparison with undifferentiated cells (Fig. 1F). As expected, AGPAT2 mRNA was undetectable in *Agpat2*<sup>-/-</sup> cells. *Ucp1* is an accepted *bona fide* marker of brown adipocyte cell identity [13,21]. UCP1 was undetectable at the mRNA and protein levels in preadipocytes (day 0 of differentiation) of both genotypes but it was present in differentiated wild type brown adipocytes since the third day of differentiation (Fig. 1G). Importantly, UCP1 remained undetectable in differentiated *Agpat2*<sup>-/-</sup> brown adipocytes at all the studied times (Fig. 1G). To promote *Ucp1* expression, we activated  $\beta$  adrenergic receptors with isoproterenol. This intervention elevated *Ucp1* mRNA levels by ~30-fold in wild type differentiated brown adipocytes compared to unstimulated cells but it was completely ineffective in *Agpat2*<sup>-/-</sup> cells (Fig. 1H).

These results indicate that after a differentiation procedure that is able to induce *Ucp1* expression in wild adipocytes, *Agpat2*<sup>-/-</sup> preadipocytes acquire some features of mature adipocytes, including LDs accumulation and *Plin1* and *Adipoq* expression, the absence of AGPAT2 totally prevents expression of *Ucp1*. Therefore, these findings suggest that AGPAT2 is required for brown adipogenesis *in vitro*.

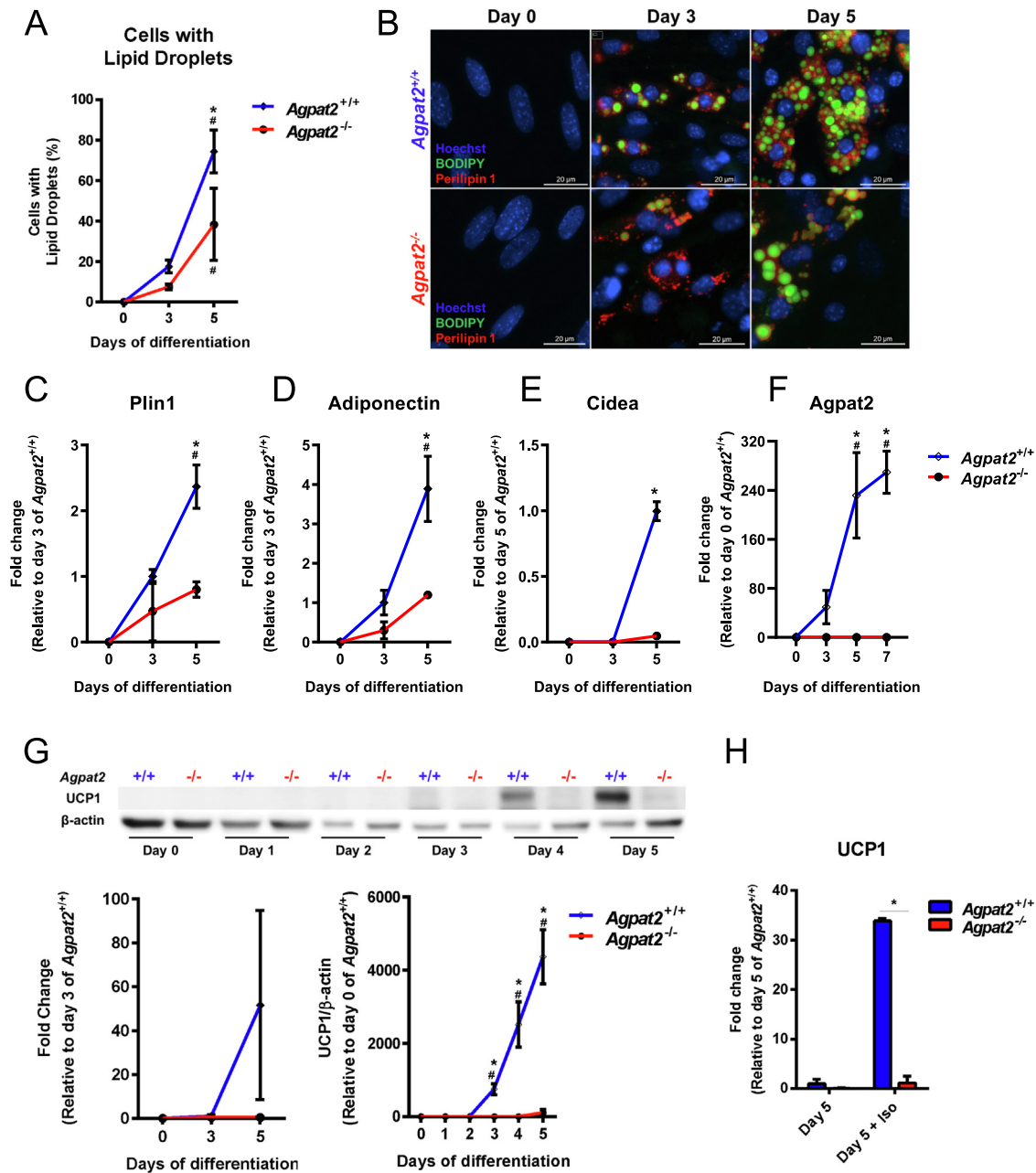


**Fig. 1.** Reduced accumulation of lipid droplets, and mRNA and protein of mature adipocyte markers in differentiated brown adipocytes of *Agpat2*<sup>-/-</sup> mice. (A) Quantification of cells with lipid droplets (BODIPY). Automated imaging analysis included ~75,000 cells in total. (B) Representative immunofluorescence images staining perilipin 1 (red), neutral lipids with BODIPY (green) and nuclei with Hoechst 33342 (blue) of wild type and *Agpat2*<sup>-/-</sup> brown adipocytes at days 0, 3 and 5 of differentiation. Scale bar 20  $\mu$ m. (C) *Plin1*, (D) *Adiponectin*, (E) *Cidea* and (F) *Agpat2* mRNA levels normalized to *36b4* and expressed as relative fold changes to wild type at day 0, 3 or 5 ( $n = 3$ ), (G) *Ucp1* mRNA levels normalized to *36b4* and expressed as relative fold changes to wild type at day 3 ( $n = 3$  per genotype) and a representative immunoblot of UCP1 and  $\beta$ -actin of differentiated brown adipocytes of wild type and *Agpat2*<sup>-/-</sup> mice at days 0–4 and 5 of differentiation and immunoblot quantification of UCP1, expressed as fold-change relative the levels of wild type mice at day 0 of differentiation and normalized to  $\beta$ -actin levels ( $n = 4$  per genotype) and (H) *Ucp1* mRNA levels of differentiated brown adipocytes of wild type and *Agpat2*<sup>-/-</sup> mice at day 5 in the presence and absence of isoproterenol (10  $\mu$ M for 6 h). Data were normalized to *36b4* and expressed as relative fold changes to wild type. Data are expressed as mean  $\pm$  SD ( $n = 3$  per genotype). \* $p < 0.05$  denote statistically significant differences between wild type and *Agpat2*<sup>-/-</sup> at the same day of differentiation, # $p < 0.05$  denotes statistically significant differences in comparison with day 0 in the same genotype.  $p$  values were calculated using two-way ANOVA.

### 3.2. Preadipocytes abundance is normal in the iBAT of newborn *Agpat2*<sup>-/-</sup> mice

Although the low proportion of lipid laden cells in differentiated *Agpat2*<sup>-/-</sup> cultures would indicate that AGPAT2 is required for adipogenesis, this observation can also be explained by a lower abundance of preadipocytes in the original SVF harvested from these mice. To study preadipocytes abundance, markers Pref1 and Zfp423 were

assessed. To track cells expressing Zfp423, a recognized marker for preadipocyte [26], *in vivo*, *Agpat2*<sup>-/-</sup>/*Zfp423*<sup>GFP</sup> mice were generated. These mice express enhanced green fluorescent protein (EGFP) under the control of *Zfp423* promoter/enhancer enabling preadipocyte mass estimation [26]. As shown in Fig. 2A, the abundance of Zfp423 expressing cells, indicated by the mass of EGFP, is equivalent in the iBAT of *Agpat2*<sup>-/-</sup>/*Zfp423*<sup>GFP</sup> and *Agpat2*<sup>+/+</sup>/*Zfp423*<sup>GFP</sup> mice. The abundance of Pref1, another protein expressed by preadipocytes but absent in

mature adipocytes, was also equivalent in the iBAT of these mice (Fig. 2A). Finally, *Pref1* abundance was also equivalent at the mRNA and protein level in cultured SVF from *Agpat2*<sup>-/-</sup> and wild type mice at the day 0 of differentiation (Fig. 2C and D).

These results show that AGPAT2 deficiency does not result in a lower abundance of preadipocytes in the iBAT nor in the SVF used in our *in vitro* adipogenesis studies. Thus, the low proportion of lipid laden cells in differentiated *Agpat2*<sup>-/-</sup> brown adipocytes is the likely result of defective adipogenic differentiation due to cell autonomous mechanisms.

### 3.3. Abundance of adipogenic transcriptional regulators *Pparγ*, *C/ebpα*, *Pparα* and *Pgc1α* but not *Prdm16* is decreased in differentiated *Agpat2*<sup>-/-</sup> brown adipocytes

We quantified key transcriptional regulators to identify potential mechanisms for the adipogenic failure of *Agpat2*<sup>-/-</sup> preadipocytes. *Pparγ* is a recognized master regulator of adipogenesis and it is essential for *Ucp1* expression as well [27]. As shown in Fig. 3A and B, the proportion of cells with nuclear labeling for *Pparγ* equally increased at the day 3 of differentiation in both *Agpat2*<sup>-/-</sup> and wild type cells. However, whereas this percentage was further increased at day 5 of differentiation in wild type cells, it remained unchanged in *Agpat2*<sup>-/-</sup> cells. In agreement with a lower proportion of *Pparγ* expressing cells, the mRNA and protein levels of PPARγ in whole cell lysates was also lower in differentiated *Agpat2*<sup>-/-</sup> cells (Fig. 3C and D). Importantly,

the proportion of lipid laden cells with simultaneous nuclear PPARγ staining was not different between wild type and *Agpat2*<sup>-/-</sup> differentiated brown adipocytes (Fig. 3E), suggesting that, irrespective of their genotype, cells expressing nuclear PPARγ are capable of building LDs during adipogenic differentiation.

PGC1α is a transcriptional co-regulator central for mitochondrial biogenesis and brown adipocyte differentiation [28,29]. As shown in Fig. 3F, PGC1α levels were lower in *Agpat2*<sup>-/-</sup> differentiated brown adipocytes at both the protein and mRNA level (days 4 and 5, respectively). *C/ebpα*, that also cooperates with PPARγ to regulate adipocyte-specific genes [30], was also lower in differentiated *Agpat2*<sup>-/-</sup> brown adipocytes at days 3 and 5 in comparison with wild type cells (Fig. 3G). Similarly, *Pparα*, a nuclear receptor that promotes fatty acid uptake, mitochondrial β-oxidation and lipoprotein metabolism [31], was decreased at the mRNA level in *Agpat2*<sup>-/-</sup> brown adipocytes at days 3 and 5 of differentiation (Fig. 3H).

PRDM16 promotes brown adipogenesis by recruiting *Pparγ* and C-terminal-binding protein-1 (CtBP1) into the regulatory regions of genes required for brown adipocyte differentiation [27,32]. In differentiating brown adipocytes of both genotypes, PRDM16 protein levels increased until the day 4 of differentiation, remaining without differences in the following days (Fig. 3I).

Together, these results indicate that the lower proportion of lipid laden cells in *Agpat2*<sup>-/-</sup> differentiated brown adipocyte cultures occurs in association with reduced levels of key transcriptional regulators for both general (*Pparγ*, *C/ebpα* and *Pparα*) and specific brown adipocyte

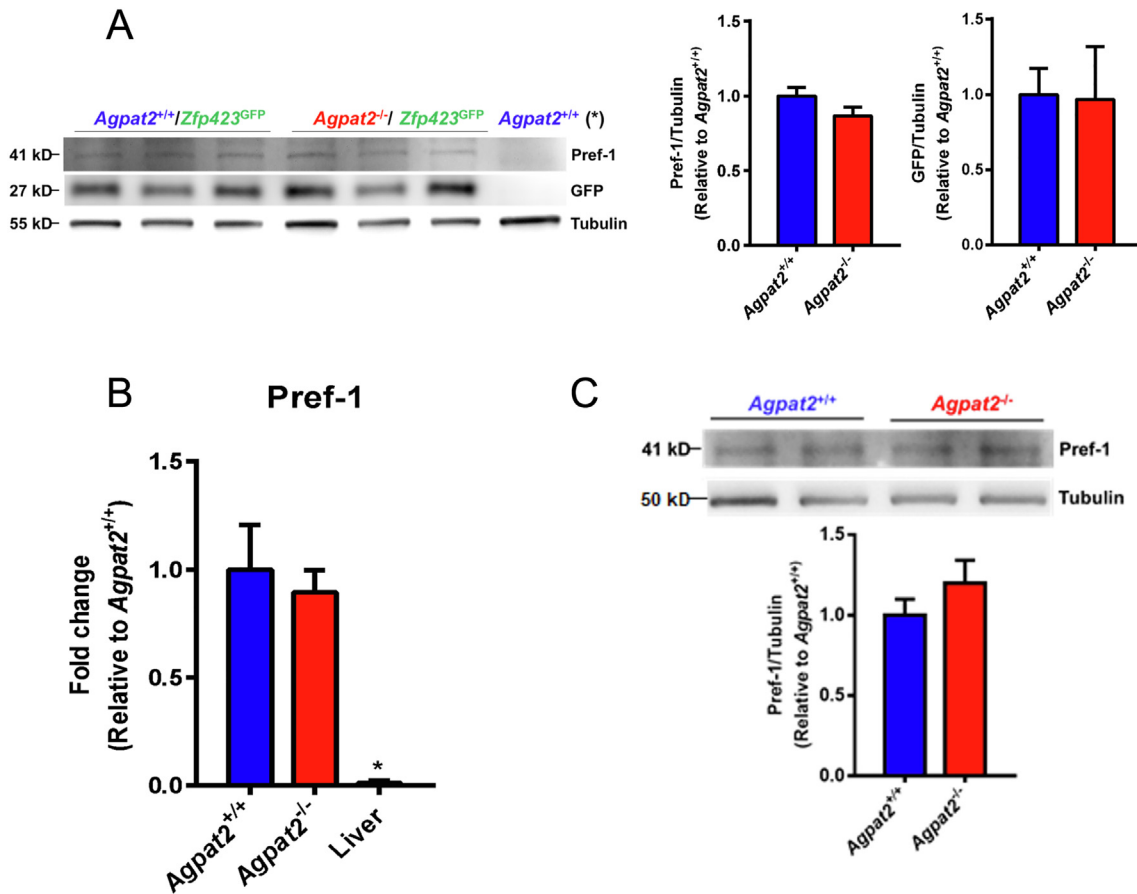


**Fig. 2.** Preadipocyte abundance is normal in the iBAT of newborn and in primary cultured stromal vascular fraction (SVF) of *Agpat2*<sup>-/-</sup> mice. (A) Representative immunoblot of PREF-1, GFP and TUBULIN in iBAT of newborn (P0.5) wild type and *Agpat2*<sup>-/-</sup> mice and immunoblot quantification of PREF-1 and GFP, expressed as fold-change relative the levels of wild type mice and normalized to tubulin levels (n = 3 per genotype). (\*): Protein sample of differentiated brown adipocytes. (B) *Pref-1* mRNA levels normalized to *36b4* and expressed as relative fold changes to wild type (n = 3 per genotype). Liver as a negative control was used. (C) Representative immunoblot of PREF-1 and tubulin in SVF of wild type and *Agpat2*<sup>-/-</sup> mice and immunoblot quantification of PREF-1, expressed as fold-change relative the levels of wild type mice and normalized to tubulin levels. Statistical analysis was performed using (A and C) two-tailed unpaired Student's *t*-tests and (B) one-way ANOVA followed by Dunnett's multiple comparisons test. \*p < 0.05 denote statistically significant differences.

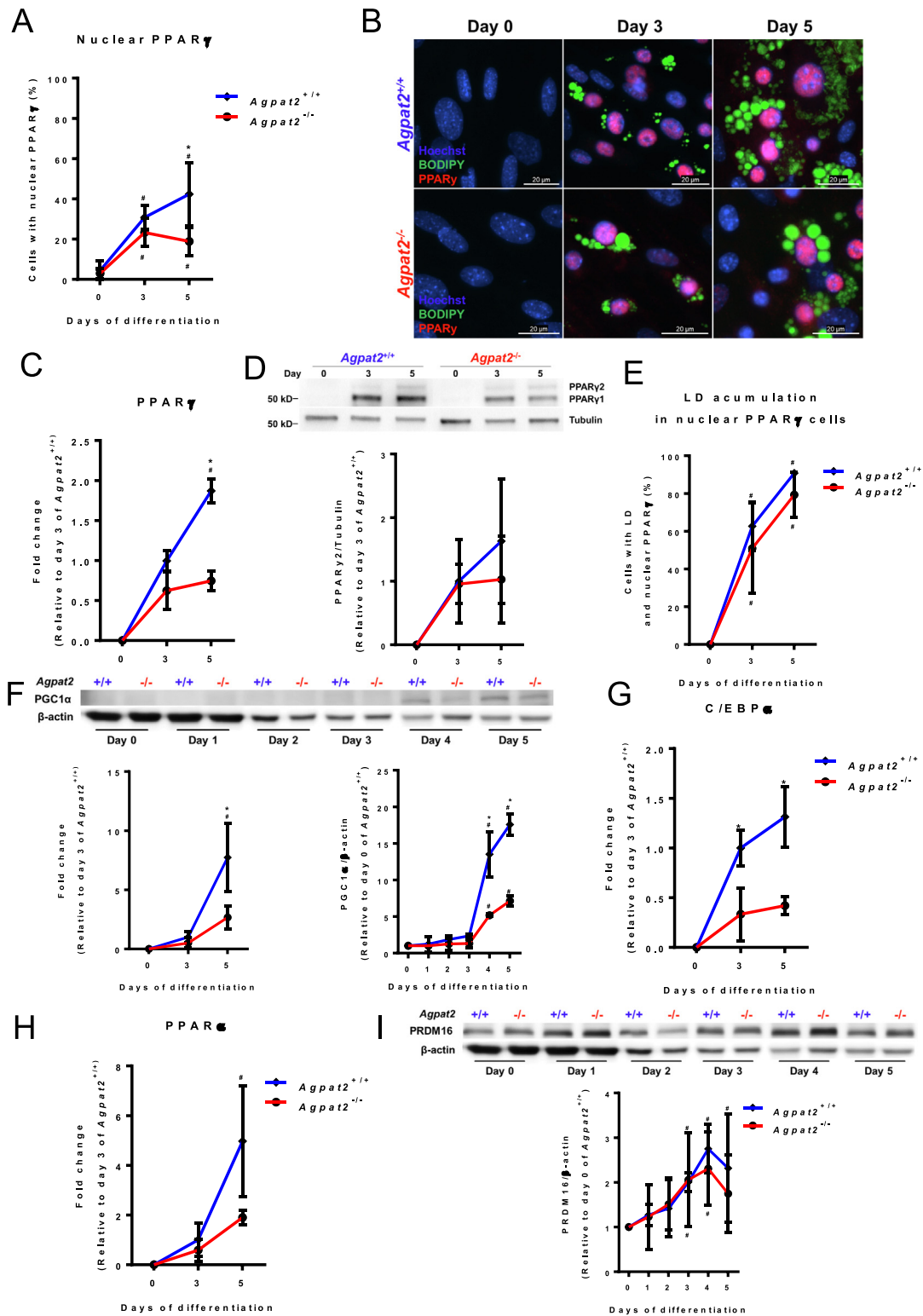


**Fig. 3.** PPAR $\gamma$  is located in the nucleus of cells that accumulate lipid droplets in differentiated brown adipocytes of wild type and  $Agpat2^{-/-}$  mice. (A) Quantification of cells with nuclear PPAR $\gamma$  protein (B) Representative immunofluorescence images stained for PPAR $\gamma$  (red), neutral lipids with BODIPY (green) and nuclei with Hoechst 33342 (blue) in differentiated brown adipocytes of wild type and  $Agpat2^{-/-}$  mice at days 0, 3 and 5 of differentiation. Scale bar 20  $\mu$ m. (C) *Ppar $\gamma$*  mRNA levels normalized to *36b4* and expressed as relative fold changes to wild type at day 3. (D) Representative immunoblot for PPAR $\gamma$  and tubulin of differentiated brown adipocytes of wild type and  $Agpat2^{-/-}$  mice at days 0, 3 and 5 of differentiation and immunoblot quantification of PPAR $\gamma$ , expressed as fold-change relative the levels of wild type mice at day 3 of differentiation and normalized to tubulin levels. Data are expressed as mean  $\pm$  SD (n = 3 per genotype). (E) Quantification of cells with lipid droplets and nuclear PPAR $\gamma$ . Automated imaging analysis included ~135,000 cells in total. (F) and (I), representative immunoblots for PGC1 $\alpha$  and PRDM16 and  $\beta$ -actin of differentiated brown adipocytes of wild type and  $Agpat2^{-/-}$  mice at days 0–4 and 5 of differentiation and immunoblot quantification expressed as fold-change relative the levels of wild type mice at day 0 of differentiation and normalized to  $\beta$ -actin levels (n = 4 per genotype). (G) *C/ebp $\alpha$*  and (H) *Ppar $\alpha$*  mRNA levels normalized to *36b4* and expressed as relative fold changes to wild type at day 0 or 3 (n = 3 per genotype). (I) *C/ebp $\alpha$*  and (H) *Ppar $\alpha$*  mRNA levels normalized to *36b4* and expressed as relative fold changes to wild type at day 0 or 3 (n = 3 per genotype). Data are expressed as mean  $\pm$  SD. \*p < 0.05 denote statistically significant differences between differentiated brown adipocytes of wild type and  $Agpat2^{-/-}$  mice at the same day of differentiation, #p < 0.05 denotes statistically significant differences in comparison with day 0 in the same genotype. p values were calculated using two-way ANOVA.

(*Pgc1α*) phenotype. Notably, total protein levels of PRDM16 do not differ between *Agpat2*<sup>-/-</sup> and wild type differentiated brown adipocytes. Importantly, although some *Agpat2*<sup>-/-</sup> cells do accumulate lipids and simultaneously have nuclear PPAR $\gamma$ , *Ucp1* remains undetectable at the protein and mRNA levels, indicating that *Agpat2*<sup>-/-</sup> preadipocytes undergo an abnormal differentiation process that fails to generate mature brown adipocytes *in vitro*.

#### 3.4. Differentiated *Agpat2*<sup>-/-</sup> brown adipocytes have increased expression of genes related to type I interferon response and lower levels of genes related to mitochondrial biogenesis/function

To further explore the transcriptional basis of the failed adipogenesis of *Agpat2*<sup>-/-</sup> cells, we performed unbiased transcriptional analysis.

Global gene expression of differentiated brown adipocytes was analyzed with microarray technology at days 0, 3 and 5 of differentiation. For this, 3 independent cell cultures were generated from individual animals and their total RNA was pooled for each genotype and time of analysis. Differentially expressed genes between wild type and *Agpat2*<sup>-/-</sup> cells were 92, 80 and 647 at days 0, 3 and 5, respectively. After 5 days of differentiation, the abundance of *Ucp1*, *Ffar4*, *Cidea* and *Cox8b* mRNAs was lower in *Agpat2*<sup>-/-</sup> adipocytes in comparison with wild type cells at the same day of differentiation (Fig. 4A). By contrast, several genes implicated in type-I interferon (IFN) response, including *Ifi44*, *Oas1g*, *Oasl2*, *Ifit1*, *Usp18* and *Ifi204* ranked among the top overexpressed genes in *Agpat2*<sup>-/-</sup> adipocytes at day 5 of differentiation (Fig. 4B).

Gene ontology (GO) analysis of differentially expressed genes revealed no differences between wild type and *Agpat2*<sup>-/-</sup> cells at days 0 and 3 of differentiation, nor in day 3 versus day 0 in both wild type and *Agpat2*<sup>-/-</sup> cells. By contrast, the comparison between day 5 and day 0 in the wild type differentiated brown adipocytes, revealed enrichment in the biological processes related to mitochondria organization (GO: 0007005), fat cell differentiation (GO: 0045444), brown fat cell differentiation (GO: 0050873) and regulation of fat cell differentiation (GO: 0045598) (Fig. 4C). In differentiated *Agpat2*<sup>-/-</sup> brown adipocytes, a relative enrichment in the same processes was observed, although to a lower magnitude to those seen in wild type cells. Interestingly, biological processes related to response to virus (GO: 0009615), cellular response to interferon-beta (GO: 0035458), response to interferon-beta (GO: 0035456) and regulation of type I interferon production (GO: 0032479), were strongly increased (Fig. 4D). This was in sharp contrast with the findings in wild type cells, in which these processes were inexistent. In fact, the comparison between wild type and *Agpat2*<sup>-/-</sup> cells at day 5 of differentiation, showed that biological processes related to response to virus (GO: 0009615), immune system process (GO:0002376) and response to interferon-beta (GO: 0035456), were significantly different between *Agpat2*<sup>-/-</sup> and wild type differentiated brown adipocytes (Fig. 4E). Many differentially expressed genes belonged to retinoic acid-inducible gene-I-like receptors (RLRs) and interferon-stimulated genes (ISGs) clusters. Among them highlight *Dhx58*, *Ifih1* and *Ddx58* in the RLRs cluster, and *Irf7*, *Usp18*, *Ifi44* and *Oas2* in the ISGs group (Fig. 4F).

A comparative analysis of cellular components between wild type and *Agpat2*<sup>-/-</sup> cells at day 5 of differentiation, showed that the expression level of genes related to mitochondrion (GO: 0005739), mitochondrial envelope (GO: 0005740), mitochondrial membrane (GO: 0031966), mitochondrial part (GO: 0044429) and mitochondrial inner membrane (GO: 0005743) were significantly decreased in *Agpat2*<sup>-/-</sup> cells (Fig. 4G). Among the genes belonging to these categories highlight *Ucp1*, *Cox8b* and *Cox7a1* (Fig. 4H).

Selected differentially expressed genes identified in the microarray analysis were quantified by RT-qPCR in a new set of differentiated brown adipocytes. *Agpat2*, *Cebpa*, *Ppara*, *Slc2a4*, *Lipin1*, *Plin5* and *Cidea* mRNA levels were quantified because their roles in adipogenic differentiation. *Elovl3* was evaluated because it is highly expressed in brown

adipocytes but is absent in white adipocytes. *Ucp1* and *Cox7a1* were tested because their roles in brown adipocyte mitochondrial function. Among the genes related to ISG we quantified *Ifit2* and *Oas2* (Fig. 4I).

As shown in Fig. 4, we corroborated that the absence of *Agpat2* determines low expression of all the evaluated genes related to brown adipocyte differentiation and specific mitochondrial processes but increases the mRNA levels of genes related to type-I IFN response.

#### 3.5. Mitochondrial morphology and mitochondria-to-lipid droplets association are altered in differentiated *Agpat2*<sup>-/-</sup> brown adipocytes

Global and targeted gene expression analyses suggest that differentiated *Agpat2*<sup>-/-</sup> adipocytes have alterations in mitochondrial biogenesis and/or function. Since mitochondrial activity is essential for both general adipogenesis and brown adipocyte phenotype [33,34], we investigated mitochondrial alterations in differentiated *Agpat2*<sup>-/-</sup> brown adipocytes. First, we examined mitochondrial ultrastructure in differentiated wild type and *Agpat2*<sup>-/-</sup> brown adipocytes at days 0 and 5 of differentiation.

Concordant with the minor transcriptomic differences noted at day 0 of differentiation (Fig. 4H), we found no differences in the mitochondrial ultrastructure between wild type and *Agpat2*<sup>-/-</sup> cells (Fig. 5A).

In wild type cells, brown adipogenic differentiation (day 5) increased mitochondrial abundance and changed the shape of these organelles, that turned from a “worm”-like to a “bean”-like morphology. Inner mitochondrial membrane ultrastructure was also modified, forming a closely packed, long parallel cristae. Interestingly, many mitochondria were intimately associated with LDs, such as no physical separation between the mitochondrial outer membrane (OMM) and the surface of LDs could be discerned (Figs. 5B and 6A).

By contrast, mitochondria in differentiated *Agpat2*<sup>-/-</sup> cells showed markedly disorganized cristae, notable for their lower density, unparallel disposition and short protrusion into the matrix, in comparison with wild type cells at the same day of differentiation (Fig. 5B). Additionally, significantly fewer mitochondria were associated to LDs in differentiated *Agpat2*<sup>-/-</sup> brown adipocytes (Fig. 6A and B).

It was recently reported that Mitofusin 2 (MFN2) [35] and Perilipin 5 (PLIN5) [36,37] are required for the physical contact between mitochondria and LDs. Although no differences in *Mfn2* mRNA content were present in our micro array analysis between differentiated *Agpat2*<sup>-/-</sup> and wild type brown adipocytes; MFN2 protein levels were progressively increased during brown adipogenic differentiation in wild type cells (~3.1, 7.5 and 8.7-fold at days 3, 5 and 7 of differentiation, respectively) (Fig. 6C). Notably, this enrichment appears to be higher than can be explained by the mere increase in mitochondrial mass, because it persisted even after normalization by mitochondrial matrix protein HSP70 levels (Fig. 6C).

*Agpat2*<sup>-/-</sup> cells showed a blunted increase in MFN2 levels during brown adipogenesis, that only reached statistical significance at the day 5 of differentiation in comparison with undifferentiated preadipocytes (~2.2-fold) (Fig. 6C). Importantly, MFN2 levels were significantly lower in differentiated *Agpat2*<sup>-/-</sup> cells compared to wild type cells after the day 5 of differentiation (Fig. 6C). However, because MFN2 levels in *Agpat2*<sup>-/-</sup> cells did not show significant differences after normalization with HSP70 during adipogenesis, this increase may be explained by a raise of mitochondrial mass in differentiated compared to undifferentiated *Agpat2*<sup>-/-</sup> cells.

Microarray analysis revealed that PLIN5 mRNA levels were ~3.4-fold lower in *Agpat2*<sup>-/-</sup> brown adipocytes in comparison with wild type adipocytes at day 5 of differentiation (Fig. 4I), suggesting that decreased levels of PLIN5 could be implicated in the defective mitochondria to LDs association in *Agpat2*<sup>-/-</sup> brown adipocytes. Quantification of mRNA levels by RT-qPCR showed that *Plin5* levels were progressively increased in wild type cells during brown adipogenesis, reaching ~7-fold increase at the day 7 of differentiation in comparison with undifferentiated preadipocytes (Fig. 6D). Differentiated *Agpat2*<sup>-/-</sup> cells had a

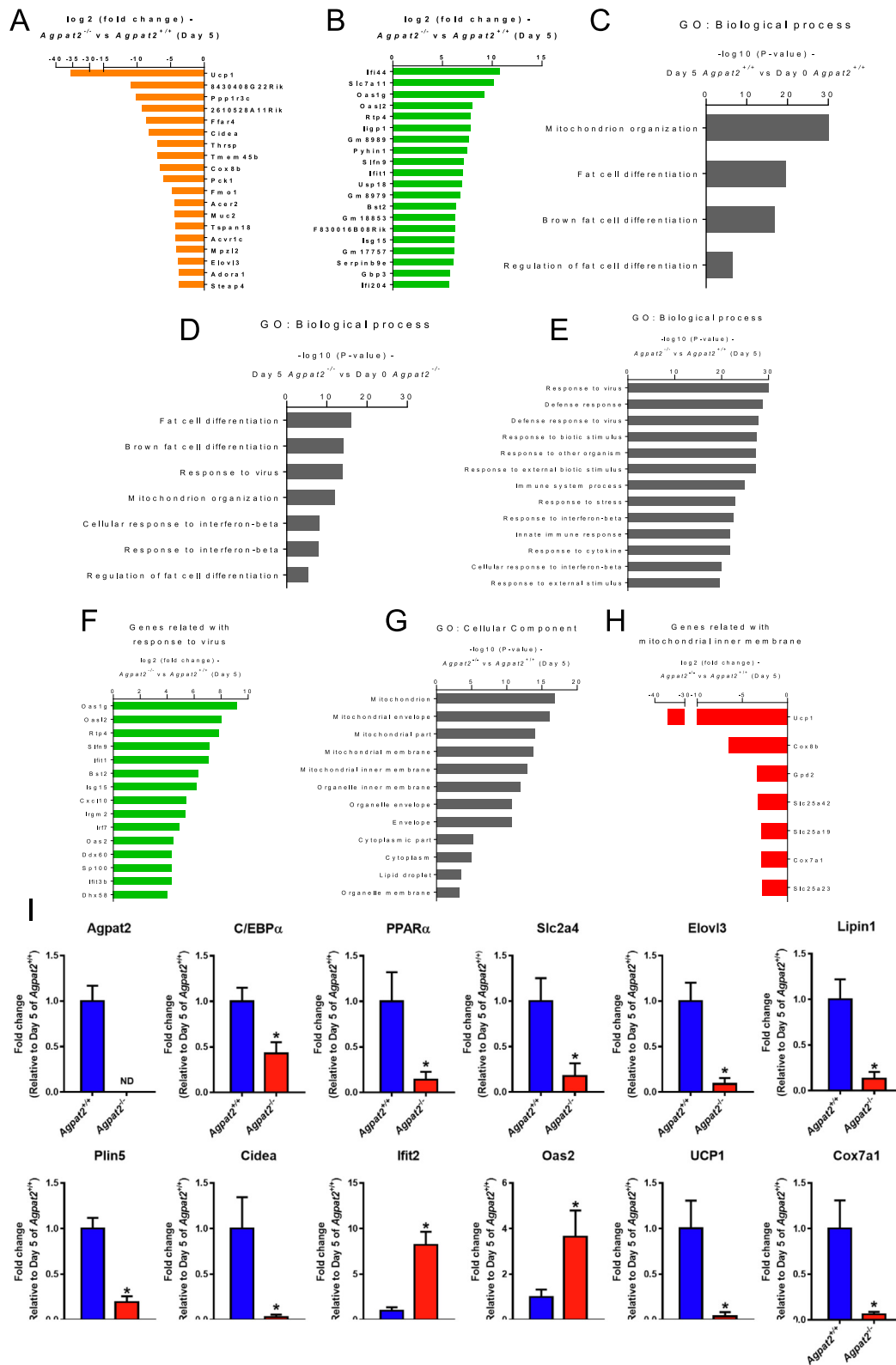


**Fig. 4.** Global gene expression analysis and RT-qPCR quantification of differentially expressed genes in differentiated brown adipocytes of  $Agpat2^{-/-}$  mice. (A)  $\log_2$  fold-change of the top 20 downregulated and (B)  $\log_2$  fold-change of the top 20 upregulated genes between differentiated brown adipocytes of wild type and  $Agpat2^{-/-}$  mice at day 5 of differentiation. Gene ontology (GO) analysis (biological process) of day 5 versus day 0 of (C)  $Agpat2^{+/+}$  and (D)  $Agpat2^{-/-}$ . GO analysis of (E) upregulated (biological process) and (G) downregulated (cellular component) genes of  $Agpat2^{-/-}$  at day 5.  $\log_2$  fold expression change of genes related with (F) cellular response to virus and (H) mitochondrial inner membrane in  $Agpat2^{-/-}$  versus  $Agpat2^{+/+}$  at day 5 of differentiation. 3 animals were used per genotype (pool). (I) mRNA levels of 1-acylglycerol-3-phosphate O-acyltransferase 2 (*Agpat2*), CCAAT enhancer binding protein  $\alpha$  (*Cebpa*), peroxisome proliferator activated receptor  $\alpha$  (*Ppara*), solute carrier family 2 member 4 (*Slc4a2*), elongation of very long chain fatty acids 3 (*Elovl3*), *Lipin1*, Perilipin 5 (*Plin5*), cell death-inducing DNA fragmentation factor, alpha subunit-like effector A (*Cidea*), uncoupling protein 1 (*Ucp1*), cytochrome c oxidase subunit 7A1 (*Cox7a1*), 2'-5' oligoadenylate synthetase 2 (*Oas2*) and interferon-induced protein with tetratricopeptide repeats 2 (*Ifit2*). Data were normalized to *36b4* and expressed as relative fold changes to wild type at day 5. ND: not detected. Data are expressed as mean  $\pm$  SD (n = 3 per genotype). Statistical analysis was performed using two-tailed unpaired Student's t-tests. \*p < 0.05 denote statistically significant differences.

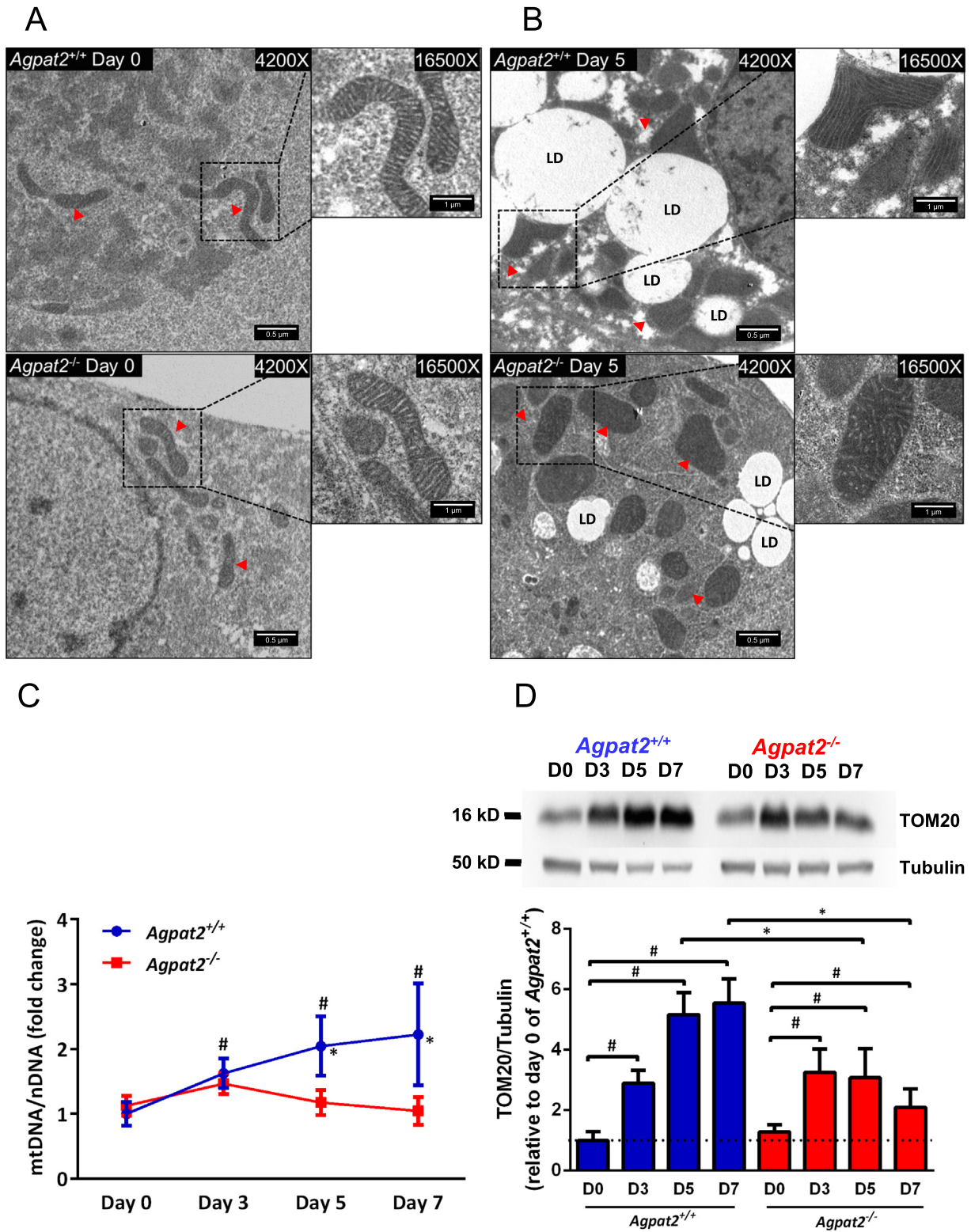


**Fig. 5.** Differentiated brown adipocytes from *Agpat2*<sup>-/-</sup> mice present an abnormal mitochondrial morphology and lower mitochondrial mass. Representative transmission electron microscopy (TEM) images from wild type and *Agpat2*<sup>-/-</sup> adipocytes at days 0 (A) and 5 (B) of brown adipogenic differentiation, respectively. Mitochondria are marked by red arrow heads. LD, lipid droplet. Scale bars indicate 0.5 and 1 μm. (C) Mitochondrial DNA copy number quantification was performed by qPCR by comparing the abundance of mtDNA-encoded *Nd4* with the abundance of nuclear DNA-encoded *Gapdh*; *n* = 8 per genotype. (D) TOM20 content in differentiated wild type and *Agpat2*<sup>-/-</sup> brown adipocytes was assessed by immunoblotting at days 0, 3, 5, and 7 of differentiation. TOM20 abundance was normalized to Tubulin and expressed as fold-change relative to wild type mice at day 0 of differentiation level. *n* = 4–5 per genotype. Data are expressed as mean ± SD. \**p* < 0.05 denote statistically significant differences between differentiated brown adipocytes of wild type and *Agpat2*<sup>-/-</sup> mice at the same day of differentiation, #*p* < 0.05 denotes statistically significant differences in comparison with day 0 of same genotype cells, *p* values were calculated using two-way ANOVA.

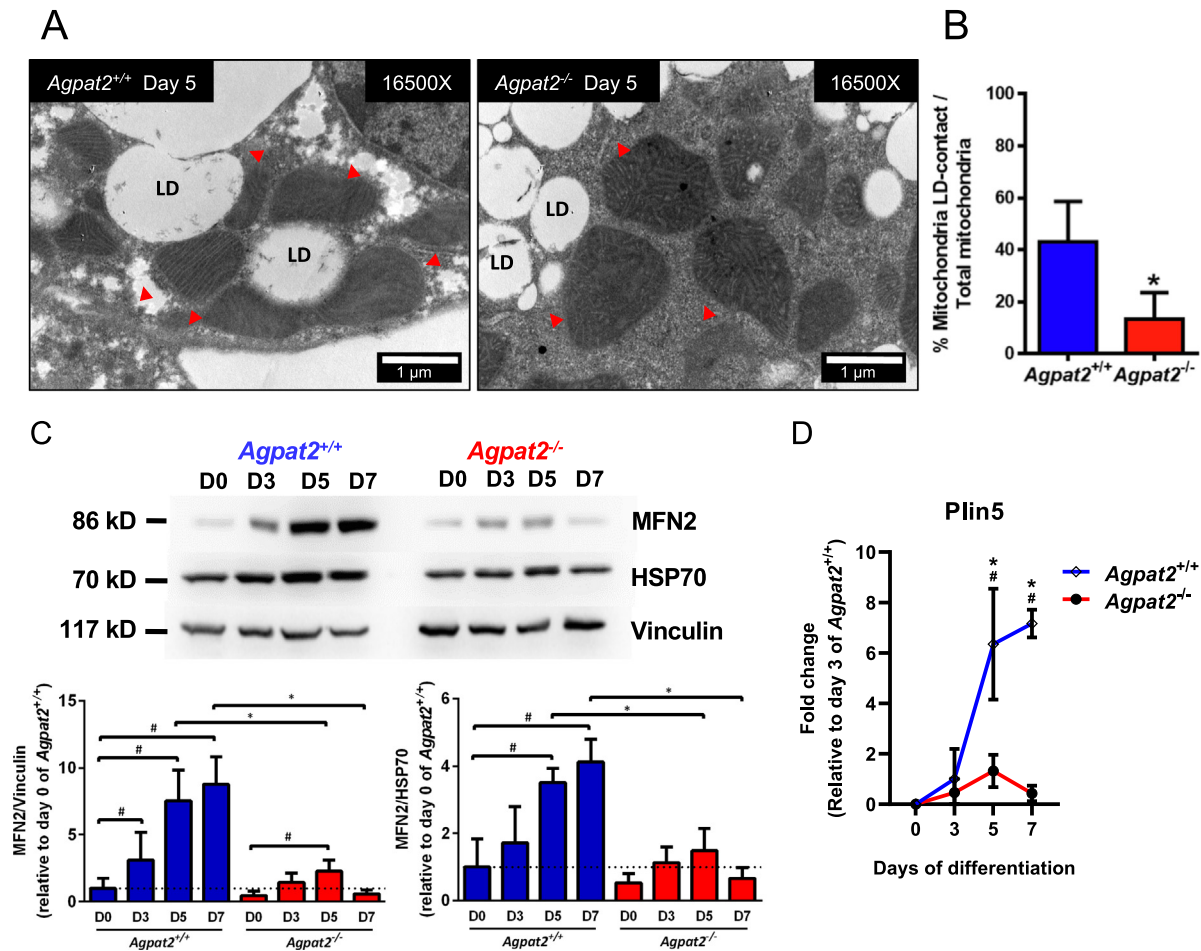


**Fig. 6.** Mitochondria-to-lipid droplet association is diminished in differentiated *Agpat2*<sup>-/-</sup> brown adipocytes. (A) Representative TEM images of differentiated wild type and *Agpat2*<sup>-/-</sup> brown adipocytes at day 5 of differentiation. Mitochondria are marked by red arrow heads. LD, lipid droplet. Scale bar indicates 1  $\mu$ m. (B) Quantification of the number of mitochondria in contact with lipid droplets (LDs) in differentiated wild type and *Agpat2*<sup>-/-</sup> brown adipocytes at day 5 of differentiation (11–14 cells were counted per genotype). (C) Representative immunoblot analysis of MFN2 in differentiated wild type and *Agpat2*<sup>-/-</sup> mice brown adipocytes at days 0, 3, 5, and 7 of differentiation. MFN2 protein levels were normalized to Vinculin and HSP70, used as cytosolic and mitochondrial loading controls respectively, and expressed as fold-change relative to wild type cells at day 0 of differentiation levels.  $n = 4$  per genotype. (D) *Plin5* mRNA levels in differentiated wild type and *Agpat2*<sup>-/-</sup> brown adipocytes at days 0, 3, 5, and 7 of differentiation. *Plin5* mRNA abundance was normalized to 36B4 mRNA levels and expressed as relative fold changes to wild type day 0.  $N = 3$ –5 per genotype. Data are expressed as mean  $\pm$  SD. \* $p < 0.05$  denote statistically significant differences between differentiated wild type and *Agpat2*<sup>-/-</sup> brown adipocytes on the same day of differentiation, # $p < 0.05$  denotes statistically significant differences in comparison with day 0 in the same genotype.  $p$  values were calculated using two-way ANOVA.

blunted raise of *Plin5* mRNA levels, that was not significantly different from the levels in undifferentiated cells (Fig. 6D).

These findings show that decreased mitochondria to LDs contacting in differentiated *Agpat2*<sup>-/-</sup> cells correlates with a lower abundance of MFN2 and PLIN5, suggesting that AGPAT2 is required for the normal physical association between mitochondria and LDs during brown adipogenesis, potentially by regulating *Mfn2* and *Plin5* gene expression.

### 3.6. Differentiated *Agpat2*<sup>-/-</sup> brown adipocytes have lower mitochondrial mass and decreased levels of enzymes involved in fatty acid beta oxidation

Our results suggest that brown adipogenic differentiation has a differential impact on the mitochondrial mass, as well as on the qualitative reorganization of inner mitochondrial membrane ultrastructure and their contacting with LDs between wild type and *Agpat2*<sup>-/-</sup> adipocytes. To assess the effect of *Agpat2* deficiency on mitochondrial mass we quantified mitochondrial DNA content by comparing the relative abundance of a mitochondrial DNA- to a nuclear DNA-encoded gene. As shown in Fig. 5C, mitochondrial to nuclear DNA ratio increased in wild type adipocytes during brown adipogenic differentiation, whereas in *Agpat2*<sup>-/-</sup> cells remaining unchanged. Therefore, mitochondrial DNA

content was significantly higher in wild type compared to *Agpat2*<sup>-/-</sup> differentiated brown adipocytes (Fig. 5C).

Because DNA copy number is not necessarily proportional to mitochondrial mass [38,39], we quantified translocase of outer mitochondrial membrane 20 (TOM20), an external mitochondrial membrane protein involved in mitochondria protein importation and a recognized marker for total mitochondrial mass [40,41]. In wild type brown adipocytes, TOM20 protein levels increased ~2.8, 5.1 and 5.5-fold at days 3, 5 and 7 of differentiation, respectively, compared to undifferentiated preadipocytes of the same genotype (Fig. 5D). TOM20 protein levels was also ~3-fold increased at day 3 of differentiation in *Agpat2*<sup>-/-</sup> adipocytes but it remained unchanged in the following days, resulting in significantly lower levels compared to wild type adipocytes at days 5 and 7 of differentiation (Fig. 5D).

Combined, these results suggest that *Agpat2* deficiency results in a lower mitochondrial mass during brown adipocyte differentiation.

Mitochondrial fatty acid beta oxidation is required for brown adipocytes thermogenic activity and it may be related to mitochondrial-to-LDs contact [42,43]. Therefore, we quantified protein levels of short-chain acyl-CoA dehydrogenase (SCAD), very long-chain acyl-CoA dehydrogenase (VLCAD) and acetyl-Coenzyme A acyltransferase 2 (ACAA2) to assess fatty acid oxidation capacity in differentiated brown

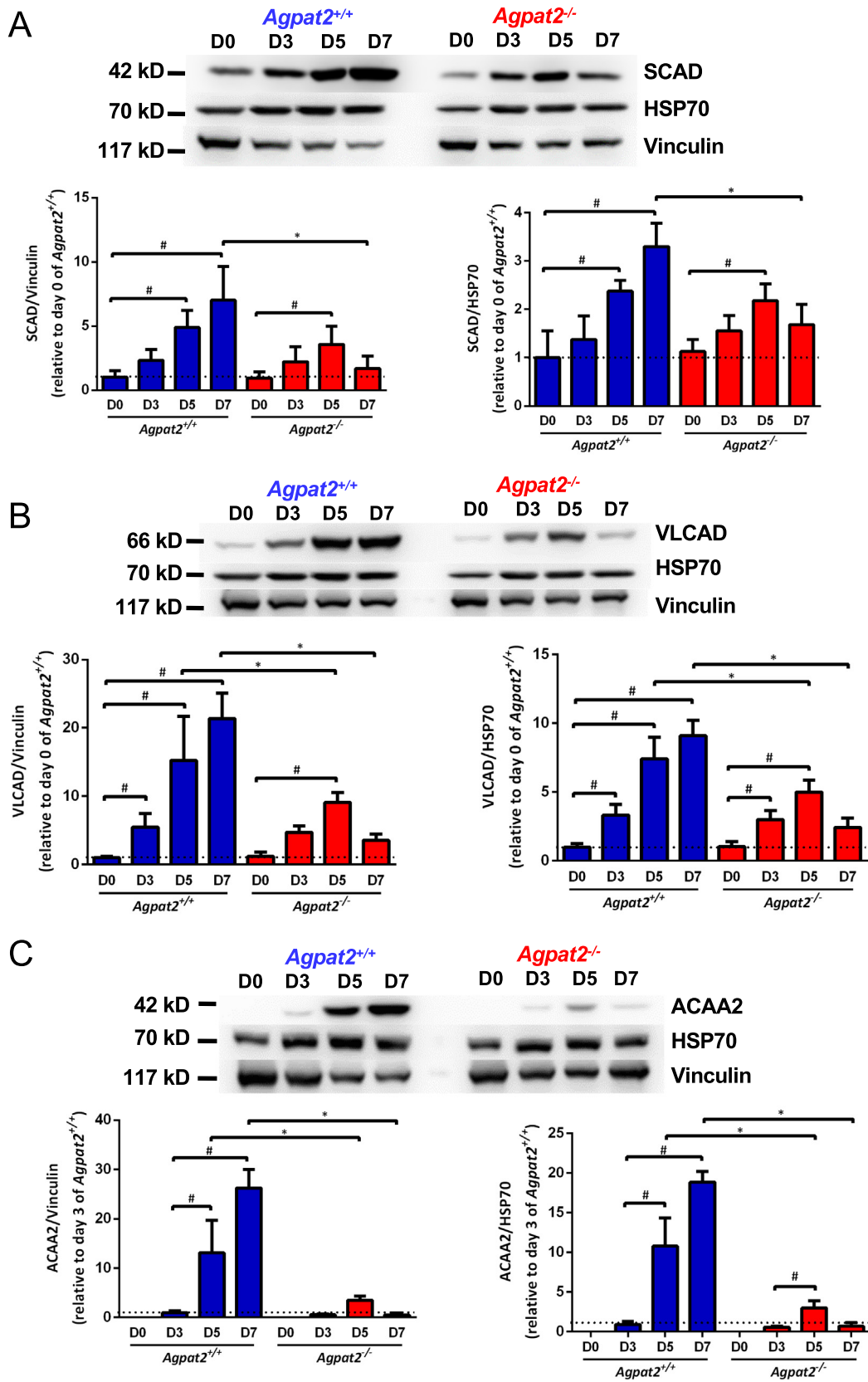


**Fig. 7.** Differentiated *Agpat2*<sup>-/-</sup> brown adipocytes have a lower abundance of enzymes implicated in fatty acid  $\beta$  oxidation. The abundance of (A) SCAD, (B) VLCAD, and (C) ACAA2 was determined by immunoblotting in differentiated wild type and *Agpat2*<sup>-/-</sup> brown adipocytes at days 0, 3, 5 and 7 of differentiation. The abundance of these enzymes was normalized to Vinculin and HSP70, used as cellular and mitochondrial loading controls, respectively, and expressed as fold-change relative to wild type cells at day 0 of differentiation levels. n = 4 per genotype. Data are expressed as mean  $\pm$  SD. \*p < 0.05 denote statistically significant differences between differentiated wild type and *Agpat2*<sup>-/-</sup> brown adipocytes at the same day of differentiation, #p < 0.05 denotes statistically significant differences in comparison with day 0 in the same genotype. p values were calculated using two-way ANOVA.

adipocytes. In wild type cells, the abundance of SCAD, VLCAD and ACAA2 progressively increased 2.3, 5.4 and 13-fold, respectively, at days 3–5 after adipogenic induction (Fig. 7A, B and C). Similar to MFN2 (Fig. 6C), this increase was higher to the raise in mitochondrial mass, because it persisted even after normalization to HSP70 levels, indicating a selective enrichment in enzymes involved in fatty acid oxidation (Fig. 7A, B and C). By contrast, brown adipogenesis determined a markedly blunted elevation in fatty acid oxidation-related enzymes in *Agpat2*<sup>-/-</sup> cells, that was particularly severe in the case of ACAA2, leading to significantly lower levels of ACAD, VLCAD and ACAA2 compared to wild type cells at the same days of differentiation.

Combined these findings indicate that *Agpat2* is required for the normal mitochondrial remodeling associated to brown adipogenesis, involving mitochondrial mass and shape, inner membrane physical configuration, abundance of fatty acid beta oxidation-related enzymes, LDs contacting and abundance of MFN2 and, possibly, PLIN5.

## 4. Discussion

### 4.1. Failed brown adipogenic differentiation in *Agpat2*<sup>-/-</sup> preadipocytes

Herein we show that differentiated *Agpat2*<sup>-/-</sup> brown adipocytes have a lower proportion of lipid-laden cells and undetectable *Ucp1*. Also, markers of mature adipocytes Cidea, Adiponectin and Perilipin1 are strongly decreased. These observations are analogous to those reported with *Agpat2*<sup>-/-</sup> MEF and iBAT preadipocytes differentiated into white adipocytes [9,10] and indicate that AGPAT2 is required for adipocyte differentiation, irrespective of their original cell lineage and final cellular phenotype.

We found equivalent proportion of cells expressing preadipocyte markers in both the iBAT of newborn mice as well as cultured stromal vascular fraction of both genotypes, thus, it is unlikely that the inability of *Agpat2*<sup>-/-</sup> differentiated cells to express brown adipocyte markers is owed to a low abundance of true brown adipocyte precursors. Therefore, we conclude that absence of AGPAT2 prevents brown adipocyte differentiation.

*Pparγ* is the master regulator of adipocyte differentiation and forms a complex with *Prdm16* and *C/ebpβ* [27,28] to promote the expression of both, white and brown adipocyte whereas *Ucp1* is a defining gene for brown adipocytes [17]. We previously showed that overexpressing *Pparγ* in white *Agpat2*<sup>-/-</sup> differentiated adipocytes, only partially reverts the adipogenic failure in these cells [9], suggesting either the existence of inhibitory post translational modifications or blocking mechanisms downstream *Pparγ* [44,45].

This hypothesis can be extended to *Prdm16*, because we also found no difference in its level between differentiated *Agpat2*<sup>-/-</sup> and wild type brown adipocytes. *Prdm16* interacts with mediator complex subunit 1 (MED1) to remodel the chromatin allowing the expression of genes related to brown differentiation as well as the expression of *Ucp1* [46,47]. Therefore, future studies will be required to determine the nature of this apparent *Prdm16* lack of function in AGPAT2 deficient adipocytes, including post translational modifications and association with transcriptional co repressors.

Our microarray analysis showed that several members of the solute carrier protein to which solute carrier 25 (*Slc25*) belongs is a nuclear-encoded protein embedded in the inner mitochondrial membrane, to which *Ucp1* (*Slc25a7*) belongs, are diminished in differentiated *Agpat2*<sup>-/-</sup> brown adipocytes, including *Slc25a19*, *Slc25a20*, *Slc25a23*, *Slc25a34*, *Slc25a35* and *Slc25a42* (Supplemental Table A1). Considering that other nuclear-encoded mitochondrial products are also decreased in these cells, such as *Cox7a1* and *Cox8b*, we speculate that the inability to express *Ucp1* in *Agpat2* deficient differentiated brown adipocytes can be due to a generalized transcriptional defect affecting the expression of mitochondrial products. This hypothesis is supported by our finding that β-adrenergic stimulation that potently increases *Ucp1* levels in wild type differentiated brown adipocytes and that is mediated by

*Pgc1α* and *Pparα*, is completely ineffective in *Agpat2*<sup>-/-</sup> differentiated cells.

*Pparα* is regulated by *Pparγ* [13], *Prdm16* [46] and early B cell factor 2 (*Ebf2*) [48] and activates the expression of *Pgc1α* in differentiated brown adipocyte, increasing *Ucp1* levels [31]. However, brown adipocytes lacking *Pparα* have normal levels of *Ucp1* [23], indicating that this nuclear receptor is not absolutely required for *Ucp1* expression. On the other hand, *Pgc1α* has a central role in mitochondrial biogenesis and cold-induced thermogenesis [31,49] and activate *Ucp1* gene promoter in response to cold exposure. Brown adipocytes lacking *Pgc1α* have low *Ucp1* levels and decreased thermogenic activation, but brown adipogenic differentiation seems to be preserved [28,50]. These antecedents suggest that both mitochondrial defects and the lack of *Ucp1* expression in *Agpat2* deficient differentiated brown adipocytes can be owed, at least partially, by low levels of *Pgc1α*.

Finally, considering that *Ucp1* is not present in *Agpat2*<sup>-/-</sup> differentiated cells a remaining question is whether these cells truly correspond to brown adipocytes or, by contrast, mostly remain as white adipocytes. Although we have no definitive answer, the actual expression of *Prdm16*, which is a recognized brown adipocyte marker, to the same levels observed in differentiated wild type cells, suggest that *Agpat2*<sup>-/-</sup> cells are able to initiate brown adipogenesis but fail to continue to more advanced stages.

Nevertheless, independent of conventional the definition of *Agpat2*<sup>-/-</sup> differentiated cells, our more important finding is that *Agpat2* is absolutely required for the expression of *Ucp1* as well as other mitochondrial proteins. Future work will be necessary for connecting the enzymatic activity of AGPAT2 with the failure of adipogenesis at the transcriptional level.

### 4.2. Abnormal expression of type I interferon response and mitochondrial biogenesis/function related genes

We also found that the mRNA abundance of ISGs is strongly induced in *Agpat2*<sup>-/-</sup> differentiated brown adipocytes. A previous study shows that deletion of *Prdm16* in brown adipose cells increased ISGs expression, including *Stat1* levels [51]. However, our results showed no differences in *Prdm16* and in *Stat1/2* nuclear levels between differentiated wild type *Agpat2*<sup>-/-</sup> brown adipocytes. Interestingly, it was found that gene deletion of activating transcription factor 7 (*Atf7*), which activates *Stat1* transcription, stimulates the expression of ISGs and inhibits adipogenesis [52]. However, we found no differences in *Atf7* expression between *Agpat2*<sup>-/-</sup> and wild type differentiated brown adipocytes (data not shown).

Finally, *Agpat2*<sup>-/-</sup> brown adipocytes showed various morphological mitochondrial defects, highlighting decreased density and organization of internal membrane cristae and lower association with lipid droplets. Mitochondrial stress enhances the expression of ISGs, including *Ifi44*, *Ifit1*, *Oasl2* and *Rtp4*, and cytoplasmic DNA and RNA sensors, such as *Ddx58*, *Ifih1* and p200 *Ifi203*, *Ifi204* and *Ifi205* family proteins [53], similar to our differentiated *Agpat2*<sup>-/-</sup> brown adipocytes. Also, mitochondrial double-stranded RNA accumulation increases the expression of ISGs and markers of immune activation (*Cxcl10*, *Ifi44*, *Ccl5*, *Ifit1*, *Cmpk2* among others) [54]. Therefore, it is plausible that defective mitochondria can be the cause of interferon response in differentiated *Agpat2*<sup>-/-</sup> brown adipocytes.

Nonetheless, the mechanisms of the increased levels of ISGs in *Agpat2*<sup>-/-</sup> brown adipocytes remains unknown as well as the role of type-I interferon response in the adipogenic failure *Agpat2* deficient cells. Further studies will be required to address these questions. We hypothesize that abnormal phospholipid composition in *Agpat2* deficient adipocytes may determine mitochondrial dysfunction that drives interferon type-I response, leading to interruption of adipogenic program as well as adipocyte cell death by lipotoxic mechanisms.

## 5. Conclusions

1. iBAT adipogenic differentiation of *Agpat2*<sup>-/-</sup> preadipocytes results in a lower proportion of lipid-laden cells and expression level of mature adipocyte markers, along with decreased levels of *Pparγ*, *Pparα*, *C/ebpα* and *Pgc1α* compared to the wild type cells. Levels of brown adipogenic regulator *Prdm16* remain unchanged.
2. Differentiated *Agpat2*<sup>-/-</sup> brown adipocytes have mitochondria qualitative abnormalities with altered morphology, decreased mass and lipid droplets association, and undetectable levels of *Ucp1*.
3. Differentiated *Agpat2*<sup>-/-</sup> brown adipocytes have a selective enrichment of interferon type I response-related gene expression. Although the mechanisms for this phenomenon remain to be determined, we proposed that mitochondrial dysfunction is an underlying cause. Similarly, we hypothesize that elevated levels of ISGs may interfere with brown adipogenic differentiation of *Agpat2*<sup>-/-</sup> preadipocytes. Supplementary data to this article can be found online at <https://doi.org/10.1016/j.metabol.2020.154341>.

## CRedit authorship contribution statement

**Pablo J. Tapia:** Conceptualization, Methodology, Validation, Formal analysis, Investigation, Writing - original draft, Writing - review & editing. **Ana-María Figueroa:** Investigation, Formal analysis, Resources, Writing - review & editing. **Verónica Eisner:** Methodology, Writing - review & editing. **Lila González-Hódar:** Resources. **Fermín Robledo:** Formal analysis. **Anil K. Agarwal:** Resources, Writing - review & editing. **Abhimanyu Garg:** Resources, Writing - review & editing. **Víctor Cortés:** Conceptualization, Resources, Methodology, Writing - original draft, Writing - review & editing, Supervision, Project administration.

## Declaration of competing interest

The authors declare no conflict of interest.

## Acknowledgments

We thank Dr. Jaime Melendez and Facultad de Química y Farmacia of the Pontificia Universidad Católica de Chile for enabling access to Cytation 5 Cell Imaging Multi-Mode Reader system (Fondequip EQM160042). We also want to acknowledge the important help of Kelly Cautivo for her skillful and constructive criticism and to Susan Smalley for her support in HCS image analysis.

## Funding

V.C. was funded by FONDECYT grant (1181214, Chile). P.J.T. was supported by CONICYT Doctoral Scholarship (21120329, Chile). V.E. was funded by a FONDECYT grant (1991770, Chile). A.M.F. was supported by ANID Doctoral Scholarship (21171743, Chile). L.G.H. was supported by CONICYT Scholarship (21171491, Chile). F.R. was supported by CONICYT Doctoral Scholarship (21171571, Chile). A.G. and A.K.A. were supported by Southwestern Medical Foundation.

## References

- [1] Agarwal AK, Garg A. Congenital generalized lipodystrophy: significance of triglyceride biosynthetic pathways. *Trends Endocrinol Metab.* 2003;14:214–21. [https://doi.org/10.1016/S1043-2760\(03\)00078-X](https://doi.org/10.1016/S1043-2760(03)00078-X).
- [2] Garg A. Acquired and inherited lipodystrophies. *N Engl J Med.* 2004;350:1220–34. <https://doi.org/10.1056/NEJMra025261>.
- [3] Garg A. Lipodystrophies: genetic and acquired body fat disorders. *J Clin Endocrinol Metab.* 2011;96:3313–25. <https://doi.org/10.1210/jc.2011-1159>.
- [4] Patni N, Garg A. Congenital generalized lipodystrophies - new insights into metabolic dysfunction. *Nat Rev Endocrinol.* 2015;11:522–34. <https://doi.org/10.1038/nrendo.2015.123>.
- [5] Garg A, Wilson R, Barnes R, Arioglu E, Zaidi Z, Gurakan F, et al. A gene for congenital generalized lipodystrophy maps to human chromosome 9q34. *J Clin Endocrinol Metab.* 1999;84:3390–4. <https://doi.org/10.1210/jcem.84.9.6103>.
- [6] Yamashita A, Hayashi Y, Matsumoto N, Nemoto-Sasaki Y, Oka S, Tanikawa T, et al. Glycerophosphate/acylglycerophosphate acyltransferases. *Biology (Basel).* 2014;3:801–30. <https://doi.org/10.3390/biology3040801>.
- [7] Agarwal AK, Arioglu E, de Almeida S, Akkoc N, Taylor SI, Bowcock AM, et al. AGPAT2 is mutated in congenital generalized lipodystrophy linked to chromosome 9q34. *Nat Genet.* 2002;31:21–3. <https://doi.org/10.1038/ng880>.
- [8] Cortés VA, Curtis DE, Sukumaran S, Shao X, Parameswara V, Rashid S, et al. Molecular mechanisms of hepatic steatosis and insulin resistance in the AGPAT2-deficient mouse model of congenital generalized lipodystrophy. *Cell Metab.* 2009;9:165–76. <https://doi.org/10.1016/j.cmet.2009.01.002>.
- [9] Cautivo KM, Lizama CO, Tapia PJ, Agarwal AK, Garg A, Horton JD, et al. AGPAT2 is essential for postnatal development and maintenance of white and brown adipose tissue. *Mol Metab.* 2016;5:491–505. <https://doi.org/10.1016/j.molmet.2016.05.004>.
- [10] Fernández-Galilea M, Tapia P, Cautivo K, Morselli E, Cortés VA. AGPAT2 deficiency impairs adipogenic differentiation in primary cultured preadipocytes in a non-autophagy or apoptosis dependent mechanism. *Biochem Biophys Res Commun.* 2015;467:39–45. <https://doi.org/10.1016/j.bbrc.2015.09.128>.
- [11] Wang W, Seale P. Control of brown and beige fat development. *Nat Rev Mol Cell Biol.* 2016;17:691–702. <https://doi.org/10.1038/nrm.2016.96>.
- [12] Kajimura S, Seale P, Spiegelman BM. Transcriptional control of brown fat development. *Cell Metab.* 2010;11:257–62. <https://doi.org/10.1016/j.cmet.2010.03.005>.
- [13] Shapira SN, Seale P. Transcriptional control of brown and beige fat development and function. *Obesity.* 2019;27:13–21. <https://doi.org/10.1002/oby.22334>.
- [14] Krahmer N, Farese RV, Walther TC. Balancing the fat: lipid droplets and human disease. *EMBO Mol Med.* 2013;5:905–15. <https://doi.org/10.1002/emmm.201100671>.
- [15] Olzmann JA, Carvalho P. Dynamics and functions of lipid droplets. *Nat Rev Mol Cell Biol.* 2018. <https://doi.org/10.1038/s41580-018-0085-z>.
- [16] Ghaben AL, Scherer PE. Adipogenesis and metabolic health. *Nat Rev Mol Cell Biol.* 2019;20. <https://doi.org/10.1038/s41580-018-0093-z>.
- [17] Villarroya F, Peyrou M, Giral M. Transcriptional regulation of the uncoupling protein-1 gene. *Biochimie.* 2017;134:86–92. <https://doi.org/10.1016/j.biochi.2016.09.017>.
- [18] Kozak UC, Kopecky J, Teisinger J, Enerbäck S, Boyer B, Kozak LP. An upstream enhancer regulating brown-fat-specific expression of the mitochondrial uncoupling protein gene. *Mol Cell Biol.* 1994;14:59–67. <https://doi.org/10.1128/MCB.14.1.59>.
- [19] Kalinovich AV, de Jong JMA, Cannon B, Nedergaard J. UCP1 in adipose tissues: two steps to full browning. *Biochimie.* 2017;134:127–37. <https://doi.org/10.1016/j.biochi.2017.01.007>.
- [20] Chouchani ET, Kazak L, Spiegelman BM. New advances in adaptive thermogenesis: UCP1 and beyond. *Cell Metab.* 2019;29:27–37. <https://doi.org/10.1016/j.cmet.2018.11.002>.
- [21] de Jong JMA, Larsson O, Cannon B, Nedergaard J. A stringent validation of mouse adipose tissue identity markers. *Am J Physiol Metab.* 2015;308:E1085–105. <https://doi.org/10.1152/ajpendo.00023.2015>.
- [22] Bray M-A, Carpenter A. Advanced assay development guidelines for image-based high content screening and analysis; 2004.
- [23] Lasar D, Rosenwald M, Kiehlmann E, Balaz M, Tall B, Opitz L, et al. Peroxisome proliferator activated receptor gamma controls mature brown adipocyte Inducibility through glycerol kinase. *Cell Rep.* 2018;22:760–73. <https://doi.org/10.1016/j.celrep.2017.12.067>.
- [24] Ashburner M, Ball CA, Blake JA, Botstein D, Butler H, Cherry JM, et al. Gene ontology: tool for the unification of biology. *Nat Genet.* 2000;25:25–9. <https://doi.org/10.1038/75556>.
- [25] Carbon S, Douglass E, Dunn N, Good B, Harris NL, Lewis SE, et al. The gene ontology resource: 20 years and still GOing strong. *Nucleic Acids Res.* 2019;47:D330–8. <https://doi.org/10.1093/nar/gky1055>.
- [26] Gupta RK, Mepani RJ, Kleiner S, Lo JC, Khandekar MJ, Frontini A, et al. Zfp423 expression identifies committed preadipocytes 2013;15:617–32. <https://doi.org/10.1016/j.cmet.2012.01.010.Zfp423>.
- [27] Seale P, Bjork B, Yang W, Kajimura S, Chin S, Kuang S, et al. PRDM16 controls a brown fat/skeletal muscle switch. *Nature.* 2008;454:961–7. <https://doi.org/10.1038/nature07182>.
- [28] Uldry M, Yang W, St-Pierre J, Lin J, Seale P, Spiegelman BM. Complementary action of the PGC-1 coactivators in mitochondrial biogenesis and brown fat differentiation. *Cell Metab.* 2006;3:333–41. <https://doi.org/10.1016/j.cmet.2006.04.002>.
- [29] Vega RB, Huss JM, Kelly DP. The coactivator PGC-1 cooperates with peroxisome proliferator-activated receptor alpha in transcriptional control of nuclear genes encoding mitochondrial fatty acid oxidation enzymes. *Mol Cell Biol.* 2000;20:1868–76.
- [30] Zuo Y, Qiang L, Farmer SR. Activation of CCAAT/enhancer-binding protein (C/EBP)  $\alpha$  expression by C/EBP $\beta$  during adipogenesis requires a peroxisome proliferator-activated receptor- $\gamma$ -associated repression of HDAC1 at the C/ebp  $\alpha$  gene promoter. *J Biol Chem.* 2006;281:7960–7. <https://doi.org/10.1074/jbc.M510682200>.
- [31] Hondares E, Rosell M, Díaz-Delfín J, Olmos V, Monsalve M, Iglesias R, et al. Peroxisome proliferator-activated receptor  $\alpha$  (PPAR $\alpha$ ) induces PPAR $\gamma$  coactivator 1 $\alpha$  (PGC-1 $\alpha$ ) gene expression and contributes to thermogenic activation of brown fat. *J Biol Chem.* 2011;286:43112–22. <https://doi.org/10.1074/jbc.M111.252775>.
- [32] Seale P, Kajimura S, Yang W, Chin S, Rohas LM, Uldry M, et al. Transcriptional control of brown fat determination by PRDM16. *Cell Metab.* 2007;6:38–54. <https://doi.org/10.1016/j.cmet.2007.06.001>.
- [33] Lindberg O, De Pierre J, Rylander E, Afzelius BA. Studies of the mitochondrial energy-transfer system of brown adipose tissue. *J Cell Biol.* 1967;34:293–310. <https://doi.org/10.1083/jcb.34.1.293>.
- [34] Cannon B, Nedergaard J. Brown adipose tissue: function and physiological significance. *Physiol Rev.* 2004;84:277–359. <https://doi.org/10.1152/physrev.00015.2003>.

- [35] Boutant M, Kulkarni SS, Joffraud M, Ratajczak J, Valera-Alberni M, Combe R, et al. Mfn2 is critical for brown adipose tissue thermogenic function. *EMBO J.* 2017;36:1543–58. <https://doi.org/10.15252/embj.201694914>.
- [36] Benador IY, Veliova M, Mahdavian K, Petcherski A, Wikstrom JD, Assali EA, et al. Mitochondria bound to lipid droplets have unique bioenergetics, composition, and dynamics that support lipid droplet expansion. *Cell Metab* 2018;27:869–885.e6. <https://doi.org/10.1016/j.cmet.2018.03.003>.
- [37] Veliova M, Petcherski A, Liesa M, Shirihai OS. The biology of lipid droplet-bound mitochondria. *Semin Cell Dev Biol.* 2020;1–10. <https://doi.org/10.1016/j.semcdb.2020.04.013>.
- [38] Malik AN, Czajka A. Is mitochondrial DNA content a potential biomarker of mitochondrial dysfunction? *Mitochondrion.* 2013;13:481–92. <https://doi.org/10.1016/j.mito.2012.10.011>.
- [39] Lee HC, Wei YH. Mitochondrial biogenesis and mitochondrial DNA maintenance of mammalian cells under oxidative stress. *Int J Biochem Cell Biol.* 2005;37:822–34. <https://doi.org/10.1016/j.biocel.2004.09.010>.
- [40] Wiedemann N, Pfanner N. Mitochondrial machineries for protein import and assembly. *Annu Rev Biochem.* 2017;86:685–714. <https://doi.org/10.1146/annurev-biochem-060815-014352>.
- [41] Zhang Y, Marsboom G, Toth PT, Rehman J. Mitochondrial respiration regulates adipogenic differentiation of human mesenchymal stem cells. *PLoS One.* 2013;8. <https://doi.org/10.1371/journal.pone.0077077>.
- [42] Gonzalez-Hurtado E, Lee J, Choi J, Wolfgang MJ. Fatty acid oxidation is required for active and quiescent brown adipose tissue maintenance and thermogenic programming. *Mol Metab.* 2018;7:45–56. <https://doi.org/10.1016/j.molmet.2017.11.004>.
- [43] Bohnert M. Tethering fat: tethers in lipid droplet contact sites. *Contact.* 2020;3. <https://doi.org/10.1177/2515256420908142> (2515256420908142).
- [44] de sa PM, Richard AJ, Hang H, Stephens JM. Transcriptional regulation of adipogenesis. *Compr Physiol* 2017;7:635–74. <https://doi.org/10.1002/cphy.c160022>.
- [45] Brunmeir R, Xu F. Functional regulation of PPARs through post-translational modifications. *Int J Mol Sci.* 2018;19:1738. <https://doi.org/10.3390/ijms19061738>.
- [46] Harms MJ, Lim HW, Ho Y, Shapira SN, Ishibashi J, Rajakumari S, et al. PRDM16 binds MED1 and controls chromatin architecture to determine a brown fat transcriptional program. *Genes Dev.* 2015;29:298–307. <https://doi.org/10.1101/gad.252734.114>.
- [47] Iida S, Chen W, Nakadai T, Ohkuma Y, Roeder RG. PRDM16 enhances nuclear receptor-dependent transcription of the brown fat-specific Ucp1 gene through interactions with mediator subunit MED1. *Genes Dev.* 2015;29:308–21. <https://doi.org/10.1101/gad.252809.114>.
- [48] Shapira SN, Lim H-W, Rajakumari S, Sakers AP, Ishibashi J, Harms MJ, et al. EBF2 transcriptionally regulates brown adipogenesis via the histone reader DPF3 and the BAF chromatin remodeling complex. *Genes Dev.* 2017;31:660–73. <https://doi.org/10.1101/gad.294405.116>.
- [49] Lin J, Handschin C, Spiegelman BM. Metabolic control through the PGC-1 family of transcription coactivators. *Cell Metab.* 2005;1:361–70. <https://doi.org/10.1016/j.cmet.2005.05.004>.
- [50] Lin J, Wu P-H, Tarr PT, Lindenberg KS, St-Pierre J, Zhang C, et al. Defects in adaptive energy metabolism with CNS-linked hyperactivity in PGC-1 $\alpha$  null mice. *Cell.* 2004;119:121–35. <https://doi.org/10.1016/j.cell.2004.09.013>.
- [51] Kissig M, Ishibashi J, Harms MJ, Lim H, Stine RR, Won K, et al. PRDM16 represses the type I interferon response in adipocytes to promote mitochondrial and thermogenic programming. *EMBO J.* 2017;36:1528–42. <https://doi.org/10.15252/embj.201695588>.
- [52] Liu Y, Maekawa T, Yoshida K, Muratani M, Chatton B, Ishii S. The transcription factor ATF7 controls adipocyte differentiation and thermogenic gene programming. *IScience.* 2019;13:98–112. <https://doi.org/10.1016/j.isci.2019.02.013>.
- [53] West AP, Khoury-Hanold W, Staron M, Tal MC, Pineda CM, Lang SM, et al. Mitochondrial DNA stress primes the antiviral innate immune response. *Nature.* 2015;520:553–7. <https://doi.org/10.1038/nature14156>.
- [54] Dhir A, Dhir S, Borowski LS, Jimenez L, Teitell M, Rötig A, et al. Mitochondrial double-stranded RNA triggers antiviral signalling in humans. *Nature.* 2018. <https://doi.org/10.1038/s41586-018-0363-0>.